Free-form registration using mutual information and curvature regularization

E. D'Agostino[1], J. Modersitzki[2], F. Maes*[1], D. Vandermeulen[1],
B. Fischer[2], and P. Suetens[1]

[1] K.U.Leuven, Faculties of Medicine and Engineering, Medical Image Computing (Radiology - ESAT/PSI), UZ Gasthuisberg, Herestraat 49, B-3000 Leuven, Belgium
{Emiliano.DAgostino,Frederik.Maes}@uz.kuleuven.ac.be
[2] Universität Lübeck, Institut für Mathematik,
Wallstraße 40, 23560 Lübeck, Germany
{modersitzki,fischer}@math.uni-luebeck.de

Abstract. In this paper we present a novel 3-D free-form non-rigid registration algorithm which combines the mutual information similarity measure with a particular curvature based regularizer, which has been demonstrated to produce very satisfactory results in conjunction with the sum of squared differences distance measure. The method is evaluated for inter-subject MR brain image registration using simulated deformations and compared with a scheme that applies the same similarity measure but with a viscous fluid regularizer.

1 Introduction

Non-rigid image registration of two three-dimensional (3-D) medical image volumes involves finding the 3-D vector field of 3-D displacements that maps each point in the reference image onto its anatomically corresponding point in the template image, such that the template image can be geometrically deformed or warped to exactly match the reference image. Typical applications include atlas construction, atlas-based segmentation, shape analysis or motion estimation. Recovering the deformation field from the image data itself requires specification of a proper similarity measure for assessing the quality of the match and of a suitable regularization scheme to exclude non-realistic deformation and to assure that the problem is mathematically well-posed.

Maximization of mutual information (MMI) of corresponding voxel intensities has been demonstrated to be highly succesful for affine image registration [7] and several approaches have been proposed to extend the MMI criterion to non-rigid matching. These differ in the way mutual information (MI) is computed when varying the registration parameters and in the regularization constraints that are imposed on the deformation field. While ideally regularization should incorporate biomechanical or statistical models of tissue deformation, in practice

* F. Maes is Postdoctoral Fellow of the Fund for Scientific Research - Flanders (FWO-Vlaanderen, Belgium).

most regularization schemes for non-rigid registration are purely mathematical and can be categorized as either implicit or explicit. Implicit schemes represent the deformation field using basis functions with built-in smoothness, e.g. B-splines [10], such that the registration solution is constrained to be within a particular class of transformations. Explicit schemes on the other hand allow for free-form deformations of individual voxels, but penalize displacements that violate local smoothness. The main advantage of explicit regularization is the possibility of incorporating physical properties of the objects to be registered, like for example elasticity. Moreover, this approach is more flexible, in the sense that the set of transformations that can be recovered, is in general much larger. In addition, the numerical treatment of the explicitly regularized registration problems leads to systems of partial differential equations for which fast, stable, and efficient solvers are available.

Recently, Hermosillo *et al.* [6] and D'Agostino *et al.* [1] constructed a voxel-wise force field that allows to drive free-form registration such as to maximize MI, by deriving the gradient of MI with respect to single voxel displacements using a continuous and differentiable representation of the joint intensity histogram based on Parzen estimation. While [6] and [1] combined the MMI force-field with an elastic and a viscous fluid regularizer respectively, in this paper we apply the MMI criterion in conjunction with the curvature based regularizer presented by Fischer and Modersitzki [4] . In contrast to other regularizers, affine linear transformations are not penalized by the curvature regularizer, such that non-rigid registration is less sensitive to non-optimal affine pre-registration or may even be applied without prior affine registration. The purpose of this work is twofold: firstly, we demonstrate that the force field derived in [6, 1] can be applied succesfully to drive MMI using different regularization kernels, such that various regularizers can be investigated for a particular application in conjunction with the same MI similarity measure; secondly, we present some initial results comparing the performance of the viscous fluid and curvature based regularizers for inter-subject MR brain image registration, both allowing large deformations. Our results indicate that acceptable and comparable registration results can be obtained using different regularization schemes and different numerical solvers, such that selecting an optimal regularizer is non-trivial.

The paper is organized as follows. In Section 2 we describe the curvature based regularization scheme and the numerical solver proposed in [4] and discuss some implementation issues. In Section 3 we investigate the performance of the curvature regularizer in function of its parameters and present a quantitative comparison with the viscous fluid regularizer of [1] for recovering simulated deformations of MR brain images.

2 Method

2.1 Similarity measure

Given two image volumes R and T defined on a domain $\Omega \subset \mathbb{R}^3$ with $T(x)$ denoting the intensity of T at $x \in \Omega$, the purpose of non-rigid image registration is to find the deformation field $u : \mathbb{R}^3 \to \mathbb{R}^3$ that maps points in R onto their corresponding points in T, such that the deformed template $T_u = T(x - u(x))$, becomes similar to R. Mutual information measures the similarity between R and T_u by the Kullback-Leibler distance

$$\mathrm{MI}[R,T;u] = \int_{\mathbb{R}^2} p^{R,T_u} \log \frac{p^{R,T_u}(g_1,g_2)}{p^R(g_1)p^{T_u}(g_2)}\ d(g_1,g_2), \tag{1}$$

with $p^{R,T_u}(g_1,g_2)$ the joint intensity density of intensities g_1 in R and g_2 in T_u with marginal densities $p^R(g_1)$ and $p^{T_u}(g_2)$ respectively. Following the approach of [1], we estimate the density p^{R,T_u} by the Parzen-window density estimator $\hat{p}^{R,T}$ based on a sample Ω_d of Ω using a Gaussian Parzen-window function $\Psi_\sigma : \mathbb{R}^2 \to \mathbb{R}$ with width σ whose choice is discussed below:

$$\Psi_\sigma(g_1,g_2) = \frac{1}{2\pi\sigma} \exp\big(- \frac{g_1^2 + g_2^2}{2\sigma}\big),$$

$$\begin{aligned} p^{R,T}(g_1,g_2) \approx \hat{p}^{R,T}(g_1,g_2) &:= \frac{1}{\#\Omega_d} \sum_{x\in\Omega_d} \Psi_\sigma(g_1 - R(x), g_2 - T(x)), \qquad (2)\\ p^R(g_1) \approx \hat{p}^R(g_1) &:= \int_{\mathbb{R}} \hat{p}^{R,T}(g_1,g_2)\ dg_2,\\ p^T(g_2) \approx \hat{p}^T(g_2) &:= \int_{\mathbb{R}} \hat{p}^{R,T}(g_1,g_2)\ dg_1, \end{aligned}$$

such that

$$\mathrm{MI}[R,T;u] \approx \hat{\mathrm{MI}}[R,T;u] := \int_{\mathbb{R}^2} \hat{p}^{R,T_u} \log \frac{\hat{p}^{R,T_u}}{\hat{p}^R \hat{p}^{T_u}}\ d(g_1,g_2) \tag{3}$$

2.2 The regularizer

Different cost functionals $\mathcal{S}$ for regularization of free-form deformations have been proposed in the literature and have been evaluated by Modersitzki [8] for unimodal image registration in conjunction with the sum of squared differences similarity measure. In this paper, we focus on the so-called *curvature* regularizer $\mathcal{S}^{\mathrm{curv}}$ introduced in [4] :

$$\mathcal{S}^{\mathrm{curv}}[u] = \sum_{\ell=1}^{3} \int_\Omega (\Delta u_\ell)^2\ dx. \tag{4}$$

Apart from its smoothness, the main advantage of this regularizer is its ability to automatically correct for affine linear deformations. This is due to the fact that the smoother is based purely on second order derivatives which do not penalize affine linear transformations, i.e.,

$$\mathcal{S}^{\mathrm{curv}}[Bx + c] = 0 \quad \text{for all} \quad B \in \mathbb{R}^{3\times 3},\ c \in \mathbb{R}^3.$$

Thus, in view of the fact that an affine linear pre-registration may be suboptimal, the curvature regularizer allows for an automatic correction of the affine linear parts. Other regularizers, such as the elastic, fluid, or diffusion regularizers, do not have this feature. It has been validated that the curvature regularizer is much less sensitive to the initial position of the images to be registered [4] .

Combining the MI similarity measure and the regularization cost in a single functional, the registration problem consists of finding the deformation u which minimizes the joint criterion

$$\mathcal{J}[u] := -\hat{\mathrm{MI}}[R,T;u] + \alpha \mathcal{S}^{\mathrm{curv}}[u], \tag{5}$$

where the parameter $\alpha > 0$ controls the strength of the regularization versus the similarity of the images. The role of α is investigated in Section 3 below.

2.3 Optimization

To compute a solution for this minimization problem, we use a steepest descent method considering that the first variation of the combined functional $\mathcal{J}$ vanishes at the optimum. To this end, one has to compute the Gâteaux-derivatives of the participating functionals.

For $u \in C^0(\Omega)^3$ and for each perturbation $v \in C^0(\Omega)^3$, the Gâteaux-derivative of $\hat{\mathrm{MI}}$ as derived by Hermosillo *et al.* [6] is given by

$$d\hat{\mathrm{MI}}[R,T;u;v] = \frac{1}{\#\Omega_d} \sum_{x \in \Omega_d} \left\langle f^{R,T}(x,u(x)), v(x) \right\rangle_{\mathbb{R}^3} \tag{6}$$

where

$$f^{R,T}(x,u(x)) = [\Psi_\sigma * \partial_{g_2} L^{R,T_u}](R(x),T_u(x)) \cdot \nabla T(x-u(x)), \tag{7}$$

$$L^{R,T_u}(g_1,g_2) := 1 + \hat{p}^{R,T_u} \log \frac{\hat{p}^{R,T_u}}{\hat{p}^R \hat{p}^{T_u}},$$

and with $*$ being the convolution operator:

$$[p * q](z_1,z_2) := \int_{\mathbb{R}^2} p(z_1-g_1, z_2-g_2) q(g_1,g_2)\ d(g_1,g_2).$$

For $u \in C^4(\mathbb{R}^3)^3$ and for each perturbation $v \in C^4(\mathbb{R}^3)^3$, the Gâteaux-derivative of $\mathcal{S}^{\mathrm{curv}}$ as derived by Fischer and Modersitzki [4] is given by

$$d\mathcal{S}^{\mathrm{curv}}[u;v] = \int_\Omega \left\langle \Delta^2 u, v \right\rangle_{\mathbb{R}^3}\ dx + \sum_{\ell=1}^{3} \int_{\partial\Omega} \Delta u_\ell \left\langle \nabla v_\ell, \boldsymbol{n} \right\rangle_{\mathbb{R}^3} - v_\ell \left\langle \nabla \Delta u_\ell, \boldsymbol{n} \right\rangle_{\mathbb{R}^3}\ dx, \tag{8}$$

where $\boldsymbol{n}$ denotes the outer normal unit vector on the boundary $\partial\Omega$. Imposing the explicit boundary conditions on u and v,

$$\nabla u_\ell = \nabla \Delta u_\ell = 0 \quad \text{on} \quad \partial\Omega, \quad \ell = 1,2,3, \tag{9}$$

the boundary integrals in the expression for $d\mathcal{S}^{\text{curv}}[u;v]$ vanish and we obtain

$$d\mathcal{S}^{\text{curv}}[u;v] = \int_{\Omega} \left\langle \Delta^2 u, v \right\rangle_{\mathbb{R}^d} \; dx. \tag{10}$$

In accordance with the calculus of variations, a function $u \in C^4(\mathbb{R}^d)^d$ which minimizes the joint functional (5) has to satisfy the Euler-Lagrange equation

$$\alpha \Delta^2 u + f^{R,T}(x, u(x)) = 0 \quad \text{for all} \quad x \in \Omega \tag{11}$$

subject to the boundary condition (9), where $f^{R,T}$ is given by (7).

The Euler-Lagrange equation (11) is a fourth-order non-linear partial differential equation (PDE). It is known as the bipotential or biharmonic equation and is well understood; see, e.g. [5] . For applications in mechanics, this equation describes the displacement of a thin plate subject to the load $f^{R,T}$. In the context of image registration, the quantity $f^{R,T}$ may be seen as a force field which drives the template towards the reference subject to the physical constraints imposed by the biharmonic operator and the boundary conditions. Also, it should be noted that there is a close connection between the curvature regularizer $\mathcal{S}^{\text{curv}}$ (4) and the functional which is minimized by the so-called *thin-plate-splines*, cf., e.g., [9]. The Gâteaux-derivatives of both functionals share the same main part but differ slightly in their boundary integrals. However, this close connection offers an alternative interpretation of the minimizer of (5). The final displacement is as smooth as thin-plate-splines but its shape is not determined by any user supplied landmarks, merely it is automatically designed by the forces imposed by the MI measure.

2.4 Implementation

The MI force field (7) depends on the width σ of the Gaussian Parzen-window kernel. A proper value for σ is determined as $\sigma = \max\{\sigma^R, \sigma^T\}$, with σ^R and σ^T estimated for R and T separately as the kernel widths that maximize the log-likelihood of the marginal densities $p^R_\sigma(g)$ and $p^T_\sigma(g)$ respectively, constructed by the Parzen-window estimator using a leave-one-out approach:

$$\begin{aligned}
p^R(g) &= c_h \cdot \#\{x : \; R(x) = g\}, \\
p^R_\sigma(g) &= \frac{c_\sigma}{\#\Omega(g)} \sum_{x \in \Omega(g)} \psi_\sigma(g - R(x)) = \frac{c_\sigma}{c_h \cdot \#\Omega(g)} \sum_{q \neq g} h^R(q) \cdot \psi_\sigma(g - q), \\
\sigma^R &= \arg\max_\sigma \sum_{g \in G} p^R(g) \log p^R_\sigma(g).
\end{aligned}$$

where $\Omega(g) := \{x \in \Omega_d : \; R(x) \neq 0 \wedge R(x) \neq g\}$, ψ_σ is a one-dimensional Gaussian, and the constants c_h and c_σ are chosen such that $\sum_{g \in G} h^B(g) = 1$ and $\sum_{g \in G} h^B_\sigma(g) = 1$, respectively, and likewise for σ^T. This approach is identical to the one described in [1].

We solve the Euler-Lagrange equation (11) by applying a semi-implicit discrete time-marching algorithm

$$\frac{u^{(k+1)}(x) - u^{(k)}(x)}{\tau} + \alpha\Delta^2 u^{(k+1)}(x) = -f^{R,T}(x, u^{(k)}(x)) \quad \text{for all} \quad x \in \Omega,$$

with τ a time-step parameter and k the iteration number. Using a finite difference approximation for the spatial derivatives, we end up with a linear system of equations involving the coefficient matrix A^{curv} which is highly structured and allows for fast solution schemes. As pointed out in [8, §12], a discrete cosine transformation can be used to diagonalize this matrix, such that the overall complexity of the solver is $\mathcal{O}(N \log N)$, with N the number of voxels. Since we solve the linear system directly and up to machine precision at each iteration, we do not need stopping rules or a convergence analysis as would be necessary for alternative iterative solution schemes, such as Multigrid, Conjugate Gradient, or SOR-like approaches.

A proper choice for the regularization parameter α depends on the order of magnitude of the forces $f^{R,T}$ and is investigated in Section 3 below. The time step τ is adjusted at each iteration such that the maximal voxel displacement $\max_x |u^{(k+1)}(x) - u^{(k)}(x)|$ is smaller than $\Delta u = 1$ voxel. Regridding and template propagation are used as in [1] to assure that the Jacobian of the deformation field is non-negative such that topology is preserved.

The method was implemented in Matlab, with image resampling, histogram computation and discrete cosine transformation coded in C.

3 Validation

We evaluated the performance of the method using the validation approach of [1] and compared it with the viscous fluid regularizer described in [1]. This approach solves

$$\nabla^2 v + \nabla(\nabla v) + f^{R,T}(x, u(x)) = 0 \quad \text{for all} \quad x \in \Omega \tag{12}$$

with $f^{R,T}$ the force field (7) and v the deformation velocity experienced by a particle at position x. An approximate solution of (12) is obtained by convolution with a Gaussian kernel ψ_γ:

$$v = \psi_\gamma \star f^{R,T} \tag{13}$$

with the spatial extent γ of the kernel controling the smoothness of the deformation. The deformation field $u^{(k+1)}$ at iteration $(k+1)$ is found by integration over time:

$$\Delta u^{(k)} = v^{(k)} - \sum_{\ell=1}^{3} v_\ell^{(k)} \left[\frac{\partial u^{(k)}}{\partial x_\ell}\right], \tag{14}$$

$$u^{(k+1)} = u^{(k)} + \Delta u^{(k)} \cdot \tau \tag{15}$$

For implementation details, we refer to [1].

Both methods were applied to simulated images generated by the BrainWeb MR simulator [2], which were non-rigidly deformed by known deformation fields u^*. These were generated by matching the T1-weighted BrainWeb image to real T1-weighted images of three periventricular leukomalacia patients, typically showing enlarged ventricles, using the viscous fluid scheme (12). The T1 and T2-weighted BrainWeb images were deformed by u^* and the original T1-weighted image was matched to the artificially deformed images using both methods. The recovered deformation u and the ground truth u^* were compared by their root mean square (RMS) error Δu evaluated in millimeter over all brain voxels Ω_B:

$$\delta u = \sqrt{\frac{1}{\Omega_B} \sum_{x \in \Omega_B} (u(x) - u^*(x))^2} \qquad (16)$$

Figure 1 illustrates the T1/T1 registration results obtained with the curvature based regularizer with $\alpha = 55$ and with the viscous fluid regularizer with $\gamma = 3$. Error values for 3 different cases are summarized in Table 1. The deformation fields obtained with $\alpha = 55$ and $\alpha = 150$ are shown in Figure 2, illustrating the smoothing effect of increasing α. Figure 3(a) plots the MI registration criterion during iterations for the curvature based regularizer. Final values of MI are 1.89 and 1.73 for $\alpha = 55$ and $\alpha = 150$ respectively. Subsequent iterations with no change in the MI criterion indicate that regridding is performed to maintain grid topology. Figure 3(b) plots the registration error obtained for the experiment in Figure 1 with the curvature based regularizer as a function of α. The error is minimal around $\alpha = 55$ and gradually increases when α is increased and more smoothing is applied.

4 Discussion

A novel free-form registration algoritm is presented that combines the MI similarity measure of [1] with the curvature based regularizer of [4] and which is implemented using a stable and fast $\mathcal{O}(N \log N)$ iterative scheme. The curvature regularizer has the advantage not to penalize affine linear transformations and was found in [4] to outperform the elastic and fluid approaches in combination with the sum of squared differences distance measure. The method was evaluated against the viscous fluid regularizer presented in [1] using artificially

Table 1. Root mean square error Δu 16 in voxels for T1/T1 and T1/T2 registrations in three different cases using the curvature based scheme C presented here and the viscous fluid scheme V of [1].

	T1/T1		T1/T2	
	C	V	C	V
Case 1	0.534	0.384	0.907	0.577
Case 2	0.612	0.304	0.769	0.443
Case 3	0.807	0.351	1.160	0.505

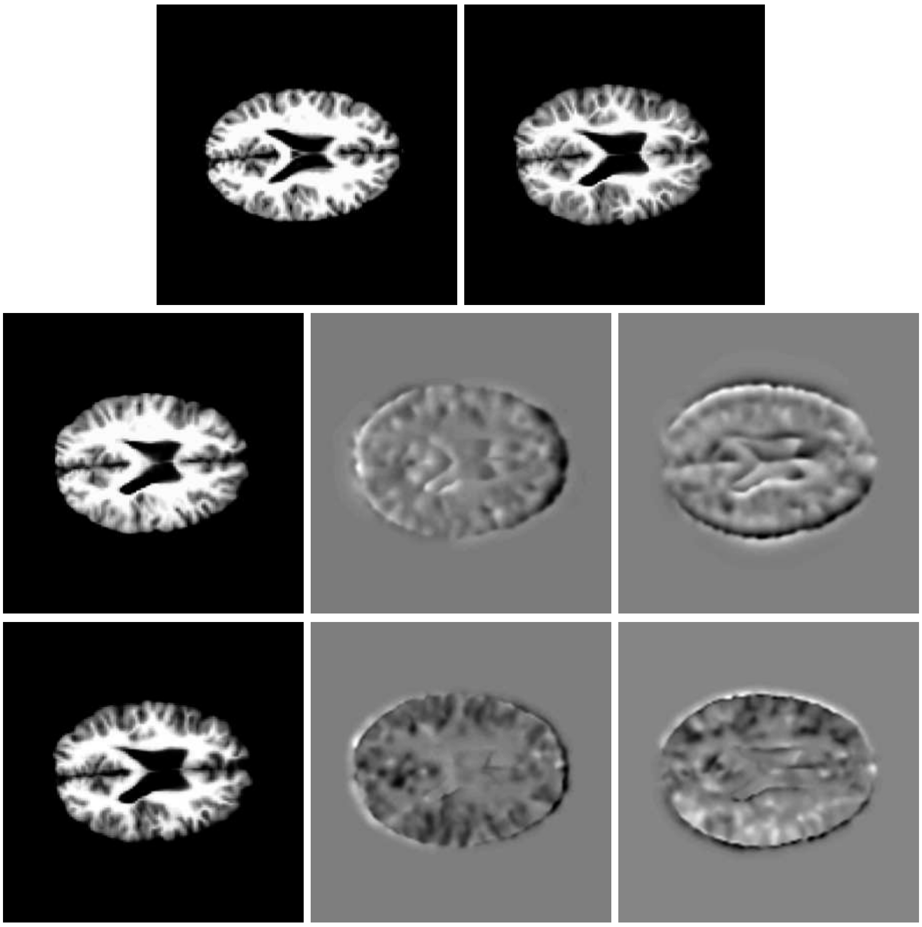

Fig. 1. Top: T1-weighted template image (left) and artificially deformed target image (right). Middle: Template matched to target using the curvature based regularizer with $\alpha = 55$ (left) and difference between ground truth and recovered deformations image (middle: horizontal component; right: vertical component). Bottom: Idem for the viscous fluid regularizer with $\gamma = 3$.

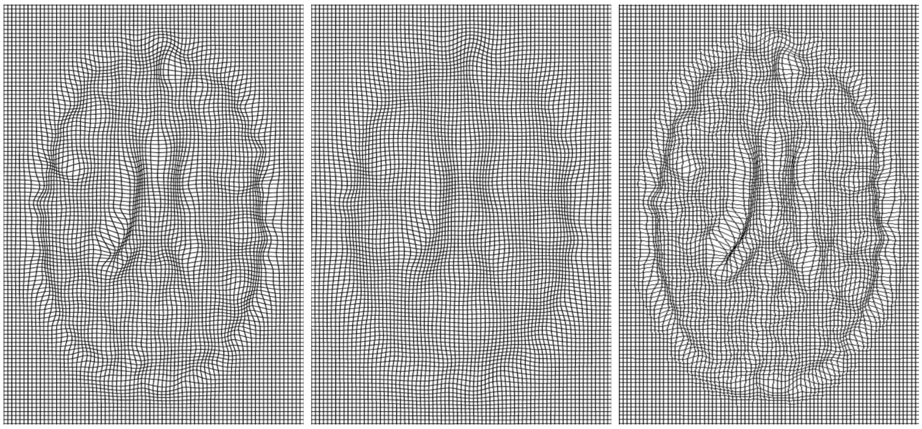

(a) (b) (c)

Fig. 2. Recovered deformation fields for the experiment of Figure 1 using the curvature based regularizer with $\alpha = 55$ (a) and $\alpha = 150$ (b) and using the viscous fluid regularizer with $\gamma = 3$ (c).

deformed images, with the ground truth deformations generated by the viscous fluid scheme.

As shown in Table 1, both approaches allow to recover the ground truth deformation with subvoxel RMS error in almost all experiments, both for T1/T1 as well as for T1/T2 registration. In general, smaller errors were obtained with the viscous fluid scheme which also generated the ground truth deformation. However, computing the ground truth deformation with the curvature based scheme for the first case T1/T1 registration yields errors of 0.539 and 1.253 voxels for the curvature and viscous fluid regularizers respectively. As illustrated in Figure 2, the curvature based regularizer yields smoother deformation fields than the viscous fluid scheme, which can be explained by the fact that the curvature constraint penalizes the second order derivatives of the deformation field. The curvature scheme can be tuned by the regularization parameter α. We studied the influence of this parameter α, determining the trade-off between smoothness of the solution and similarity with respect to the known solution.

Our results demonstrate that different regularization schemes can be applied in conjunction with the same MMI driving force field as described above, which may generate equivalent registration results. Future work will focus on evaluating the ability of different schemes to generate consistent deformations that would allow to construct statistical deformation models.

References

1. E. D'Agostino, F. Maes, D. Vandermeulen, P. Suetens. A viscous fluid model for multimodal non-rigid image registration using mutual information. *MICCAI 2002*, Tokyo, 23-26 September, 2002.

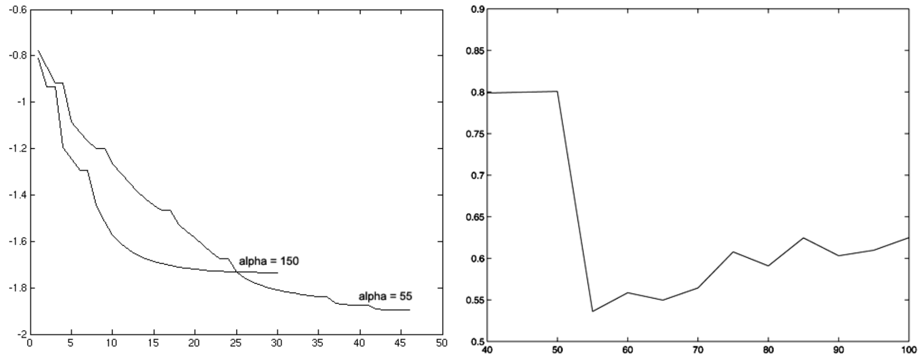

(a) (b)

Fig. 3. (a) Mutual information registration criterion over iterations for curvature based regularizer with $\alpha = 55$ and $\alpha = 150$; (b) Registration error (in voxels) for the experiment of Figure 1 for the curvature based regularizer with α varying between 10 and 100.

2. BrainWeb MR simulator. Available at http://www.bic.mni.mcgill.ca/brainweb/.
3. B. Fischer and J. Modersitzki. A unified approach to fast image registration and a new curvature based registration technique. Preprint a-02-07, Institute of Mathematics, Medical University of Lübeck, 2002.
4. B. Fischer and J. Modersitzki. Curvature based image registration. *JMIV*, 18(1):81–85, 2003.
5. W. Hackbusch. *Partial Differential Equations.* Teubner, Stuttgart, 1987.
6. G. Hermosillo. *Variational methods for multimodal image matching.* Phd thesis, Université de Nice, France, 2002.
7. F. Maes, A. Collignon, D. Vandermeulen, G. Marchal, and P. Suetens. Multimodality image registration by maximization of mutual information. *IEEE Trans. Medical Imaging*, 16(4):187–198, 1997.
8. J. Modersitzki. *Numerical Methods for Image Registration.* Oxford University Press, to appear 2003.
9. K. Rohr. *Landmark-based Image Analysis.* Computational Imaging and Vision. Kluwer Academic Publishers, Dordrecht, 2001.
10. D. Rueckert, L.I. Sonoda, C. Hayes, D. Hill, M.O. Leach, and D.J. Hawkes. Nonrigid registration using free-form deformations: application to breast MR images. *IEEE Trans. Medical Imaging*, 18(8):712–721, 1999.